MARMARA UNIVERSITY
INSTITUTE FOR GRADUATE STUDIES
IN PURE AND APPLIED SCIENCES

RECYCLING OF INVESTMENT CASTING SHELL MOLD SANDS IN CERAMIC INDUSTRY

SEVNUR OZDEMIR

MASTER THESIS
Department of Metallurgical - Materials Engineering

ADVISOR
Prof. Dr. Recep ARTIR

ISTANBUL, 2013

ACKNOWLEDGEMENTS

I would like to express my special thanks to my supervisor Prof. Dr. Recep ARTIR for his excellence guidance and his patience during this work.

Thanks due to my company colleagues Burcu BAGCI, Erdem YILDIRIM, Burak IZMIRLIOGLU and Melih USTUN for their great assistance during the tests performed in Sisecam Glass Research Center, and also our research assistants Burcu N. CETINER and Ismail TOPCU for their help during the tests performed in Marmara University Metallurgical and Materials Engineering laboratories.

Thanks to my husband Tolga OZDEMIR, who always encouraged me in every stage of my work and my friend Sinem YAKICI for her support by heart to complete my thesis.

CONTENTS

	PAGE
ACKNOWLEDGEMENTS	**i**
CONTENTS	**ii**
ABSTRACT	**iii**
ÖZET	**iv**
SYMBOLS	**v**
ABBREVIATIONS	**vi**
LIST OF FIGURES	**vii**
LIST OF TABLES	**viii**
1. INTRODUCTION	**1**
1.1. Investment Casting Shell Moulds Recycling Literature Survey	2
1.1.1. Materials and Methods	4
1.1.2. Results	5
2. MATERIAL AND METHOD	**13**
2.1. Sample Preparation	13
2.2. Sample Preparation for Sintering	14
3. RESULTS AND DISCUSSION	**16**
3.1. Experimental Results	16
3.1.1. XRF and XRD analysis of shell powders	16
3.1.2. Thermal behaviour analysis	18
3.1.3. Microstructural evaluation	19
3.1.4. XRD analysis of samples after firing	23
3.1.5. Some physical properties of samples after firing	26
3.1.6. Hardness of samples after sintering	29
4. CONCLUSION	**30**
REFERENCES	**31**
CURRICULUM VITAE	

ABSTRACT

RECYCLING OF INVESTMENT CASTING SHELL MOLD SANDS IN CERAMIC INDUSTRY

In this study recycling of mould sand was investigated. Firstly, to determine the compositions and microstructures of the used and unused mould wastes, XRF, XRD, EDS, SEM and DTA-TG analysis were performed. With the help of the literature survey and the analysis results, samples with 4 different compositions were prepared.

MgO addition was attempted between 0-3 wt % for densification. The compacted powder mixtures were sintered with 3 different sintering temperature at 1450, 1475 and 1500 °C for 3 hours. Sinterability of the samples were investigated and explored. Microstructural evaluation and chemical analysis were carried out by XRD, EDS, SEM, and physical properties such as bulk density, apparent porosity, hardness, water absorbtion, loss on ignition and shrinkage were also measured.

MgO addition was found to promote sinterability of mullite-zirconia composite leading to an increment in shrinkage of the samples thus bulk density increased. The shrinkage rate increased with increasing magnesia addition at all temperatures, resulted in decreasing apparent porosity.Bulk density increase with increasing magnesia addition at all temperatures caused to decrease water absorption and improvement in hardness.

MgO addition into mould sand can provide improved or better mechanical properties and reduces the sintering temperature for cost effective processing and recycling of the mould sand. MgO added investment casting waste mould sand can be partially used in some refractory applications for reinforcement purposes where operation temperature should be lower than 1500 °C.

December, 2013 **Sevnur ÖZDEMİR**

ÖZET

HASSAS DÖKÜM KALIP KUMLARININ SERAMİK SANAYİNDE YENİDEN DEĞERLENDİRİLMESİ

Bu çalışmada, hassas döküm kalıp kumlarının geri dönüşümü incelenmiştir. Öncelikli olarak, dökümde kullanılmamış ve dökümde kullanılmış kalıp kumlarının kompozisyonu ve mikroyapı özelliklerinin tespit edilebilmesi için XRF, XRD, EDS, SEM ve DTA-TG analizleri yapıldı. Literatürde yer alan çalışmalar ve analiz sonuçları doğrultusunda, sinterlemeye yardımcı olması için 1,2 ve 3 ağ%'e kadar MgO ilavesi ile 4 farklı kompozisyonda numuneler hazırlandı. 1450, 1475 ve 1500 °C sıcaklık değerlerinde 3 saat sinterlenerek özellikleri incelenmek üzere karakterize edildi. Numunelerin kimyasal ve mikroyapı özellikleri için XRD, EDS ve SEM analizleri yapıldı. Ayrıca kaba yoğunluk, görünür porozite, sertlik, su emme, ağırlık kaybı ve pişme küçülmesi gibi fiziksel özellikleri de ölçüldü.

Yapılan analizler sonucunda, MgO ilavesinin müllit-zirkon yapısında sinterlenme özelliğini arttırdığı, bu sebeple de hacimsel küçülme oranlarında düşüşe, kaba yoğunlukta artışa sebep olduğu gözlemlendi. Pişme küçülmesi oranlarının tüm ilavelerde sıcaklığa bağlı olarak, aynı sıcaklıkta MgO ilavesine bağlı olarak arttığı, görünür porozitenin de azaldığı tespit edildi. Kaba yoğunluğun MgO ile artışı, su emme oranlarında düşüşe, dolayısı ile numune sertliğinin artışına yol açtığı gözlemlendi.

Kalıp kumlarına yapılan MgO ilavesinin, malzemenin mekanik özelliklerinin iyileştirilmesine yardımcı olmasının yanında, düşük sinterlenme sıcaklıklarında çalışması nedeniyle proses ve geri dönüşüm maliyetlerinin düşük olması açısından da avantaj sağlamaktadır. MgO ilaveli hassas döküm kalıp kumları 1500 °C'nin altındaki sıcaklıklarda, bazı refrakter uygulamalarında takviye amaçlı olarak kullanılabilir.

Aralık, 2013 **Sevnur ÖZDEMİR**

SYMBOLS

K_{Ic} **:** Fracture toughness (MPa $m^{1/2}$)

T **:** Temperature (°C)

ρ **:** Relative density

ρ_f **:** Final density

ABBREVIATIONS

DTA : Differential thermal analysis

DSC : Differential scanning calorimetry

EDS : Energy-dispersive X-ray spectroscopy

SEM : Scanning electron microscopy

TG : Thermogravimetric analysis

XRD : X-ray diffraction spectroscopy

XRF : X-ray fluorescence spectroscopy

LIST OF FIGURES

PAGE

Figure 1.1- $MgO–Al_2O_3–SiO_2$ phase diagram 9

Figure 2.1- Unused and used pieces of the investment casting shell moulds 13

Figure 3.1- XRD analysis pattern of unused shell powder 17

Figure 3.2- XRD analysis pattern of used shell powder 17

Figure 3.3- TG/DSC analysis graph of unused shell powder 18

Figure 3.4- TG/DSC analysis graph of used shell powder 19

Figure 3.5- SEM micrograph of used mold powder after milling and sieving 20

Figure 3.6- Top view of the sintered samples 20

Figure 3.7- Optical microstructure photos of 2% MgO added sample , sintered at 1450°C at x150, x300, x600 magnifications 21

Figure 3.8- SEM photos of the sintered samples at 1450°C, 1475°C and 1500°C 22

Figure 3.9- SEM micrograph of 2% MgO containing sample sintered at 1500°C 22

Figure 3.10- EDS analysis of 3% MgO containing sample sintered at 1475°C 23

Figure 3.11- XRD analysis pattern of no MgO added sample at 1450°C 24

Figure 3.12- XRD analysis pattern of no MgO added sample at 1500°C 24

Figure 3.13- XRD analysis pattern of %3 MgO added sample at 1450°C 25

Figure 3.14- XRD analysis pattern of %3 MgO added sample at 1500°C 25

Figure 3.15- Bulk density variation as a function of MgO addition after sintering at 1450,1475 and 1500°C for 3 hours 26

Figure 3.16- Apparent porosity variation as a function of MgO addition after sintering at 1450,1475 and 1500°C for 3 hours 27

Figure 3.17- Water absorption variation as a function of MgO addition after sintering at 1450,1475 and 1500°C for 3 hours 27

Figure 3.18- Weight loss variation as a function of MgO addition after sintering at 1450,1475 and 1500°C for 3 hours 28

Figure 3.19- Shrinkage variation as a function of MgO addition after sintering at 1450,1475 and 1500°C for 3 hours 28

Figure 3.20- Hardness variation as a function of MgO addition after sintering at 1450,1475 and 1500°C for 3 hours 29

LIST OF TABLES

	PAGE
Table 2.1- Compositions of samples	14
Table 2.2- Sintering program for 1450°C, 1475°C and 1500°C	15
Table 2.3- Sintered sample names	15
Table 3.1- Compositions of unused and used shell powders	16
Table 3.2- Phases detected by XRD analysis of used and unused mould sand	18

1. INTRODUCTION

Investment casting is one of the oldest manufacturing processes, dating back thousands of years, in which molten metal is poured into an expendable ceramic mold. The mold is formed by using a wax pattern - a disposable piece in the shape of the desired part. The pattern is surrounded, or "invested", into ceramic slurry that hardens into the mold. Investment casting is often referred to as "lost-wax casting" because the wax pattern is melted out of the mold after it has been formed.

Investment casting can make use of most metals, most commonly using aluminum alloys, bronze alloys, magnesium alloys, cast iron, stainless steel, and tool steel. This process is beneficial for casting metals with high melting temperatures that can not be molded in plaster or metal. Parts that are typically made by investment casting include those with complex geometry such as turbine blades or firearm components. High temperature applications are also common, which includes parts for the automotive, aircraft, and military industries [1].

The investment casting process is being used extensively today as a shortcut to producing finished high quality precision parts which, otherwise would have to be made by precision machining. Complex parts with undercut and smooth surfaces, accurate dimensions and fine details can be made by investment casting. In spite the many advantages of investment casting over other procedures, the investment casting process is stil relatively time consuming and expensive. The reason for the high production cost and time is that the production is one - to - one, that means each pattern creates only one part.

In the 1940s, World War II increased the demand for precision net shape manufacturing and specialized alloys that could not be shaped by traditional methods, or that required too much machining. Industry turned to investment casting. After the war, its use spread to many commercial and industrial applications that used complex metal parts [2].

Following the good developments, the greatest problem of the investment casting industry is the investment casting mould scraps that can not be used for casting a second

piece. So each cast item is produced with an amount of mould waste besides. Those wastes are not reusable or recyclable in other industries increases the product cost, also affecting the environment seriously. In this study, our aim is to find a way to produce value added materials in ceramic industry to reduce the production cost and as well as reduce the environmental pollution.

1.1. Investment Casting Shell Moulds Recycling Literature Survey

There are only a few studies found in the literature related to investment casting shell moulds recycling. Summary of one of the studies is given below from Valenza et.al.[3]. Some articles discussed the effect of different oxides additions on sintering behaviour of ceramic materials [4-14], however very few articles studied on the effect of MgO addition on sintering behavior of mullite [5, 15-17].

In Valenza et.al.'s [3] study, powders obtained by milling ceramics shells, already used as investment material in casting processes, were sintered to investigate their possible re-use in the production of ceramic refractories. The sintering behavior of these powders, consisting essentially of silica and mullite, were analysed both in a heating run by conventional contact dilatometry and in an isothermal process via optical dilatometry. The mechanical properties of sintered composites formed with a matrix of fine powders and an inert coarse phase of the same material are evaluated and discussed in view of possible use in the production of refractory tiles.

In many industrial casting processes ceramic shells are used as investment materials. After use, a large amount of ceramic wastes are produced which in turn affects the overall production costs. The re-use of these materials in the form of powders to be used in new sintering processes could be recommendable in spite of additional milling costs.

The refractory lining in the combustion chamber of gas turbine plants is normally made of sintered tiles of traditional mullite/alumina refractory. The microstructure of such a refractory is rather heterogeneous, including coarse mullite and alumina grains (over 1 mm in size) with large macropores, bounded by a fine microporous alumina matrix. Microcracks of a size comparable with that of the coarser grains are present to

some extent throughout the matrix, sometimes crossing the mullite grains. The large amount of open porosity (beyond 18%) allows to keep low both the thermal conductivity and the weight of the tiles. As a consequence, however, the mechanical strength is very low (flexural strength around 13 MPa and fracture toughness K_{Ic} = 0.7 MPa $m^{1/2}$). During their service (typically 20,000 h between two consecutive maintenance stops) the tiles, which are normally grafted to the steel hull, undergo both thermal cycling and mechanical vibrations. On inspections during the maintenance stops, it is not infrequent to find the more exposed tiles damaged and these have to be replaced on site with difficult and expensive interventions. Typical damages are: surface degradation caused by exposure to the hot combustion gas and formation of through thickness cracks of considerable lengths which, however, are kept under control by an effect of grain bridging opposing crack propagation.

The use of powders of waste shells containing a vitreous phase could be beneficial under two aspects. On one hand, vitrification at the hot side of the tiles may protect the surface from erosive actions, while viscous flow in the refractory matrix may improve its resistance to crack propagation.

The main problem in this application of the shell waste is, however, the sinterability of the powders when used as the fine matrix of refractory composites. The large grains behave as an inert reinforcement in all cases, so that any low-cost material could be considered for this purpose, including coarser powders of the same waste.

In Valenza et.al.'s [3] study, sintering experiments in both traditional and optical dilatometry have been carried out on powders obtained from milling of waste materials. The sinterability of such powders at 1400 °C appears to be comparable to that of alumina powders of similar size and the small scale mechanical properties are compatible with those of a common refractory. An attempt also was made to obtain a refractory composite by mixing fine powders with coarse grains of the same material and sintering at 1400 °C. This composite was also tested in bending and the results are compared to the behaviour of a traditional refractory.

1.1.1. Materials and Methods

In Valenza et.al.'s [3] study, all samples were prepared starting from a waste ceramic material based on molochite whose phase composition derived from EDS and XRD spectra is: 53 wt.% vitreous SiO_2 , 45 wt.% mullite, 0.7 w t.% Fe_2O_3 and 1.3 wt.% K_2O.

Fine powders (1–10 mm), obtained from this ceramic material have been used to create samples for sintering tests; a slurry, obtained by addition of Polyvinylpyrrolidone as a lubricant, has been uniaxially pressed to get cylindrical samples. Before the experimental tests, samples were pre-heated at 450°C for 2 h in order to remove any organic compounds; a slow heating /cooling rate (3°C /min) was used to avoid thermal stress or forced gas release. Their green relative density, measured by the Archimede's technique, is 0.69.

The sintering behaviour was analysed both during heating with a linear temperature ramp via conventional dilatometry and in an isothermal process via optical dilatometry. The latter technique allows not only to use larger samples but also to avoid any compression of the sample by the dilatometer rod.

These tests have been performed in a tubular furnace which allows to introduce the sample in a very short time, typically 30s, when all process parameters are stable; in this way a quasi-isothermal heating process can be simulated. During the tests, the sample profile is monitored continuously in order to acquire images and subsequently measure any change in diameter. The diameters are calculated for surface tension and contact angle measurements.

Moreover, a set of cylindrical samples have been sintered in a muffle furnace at 1350°C reaching a final relative density of 0.77; these specimens were mechanically tested in radial compression to determine the tensile strength.

Finally, in Valenza et.al.'s [3] study, to evaluate the feasibility to produce a refractory with improved characteristics from this molochite based waste material, a composite was made by slip casting mixing together 20% of fine powder (1–10 μm), 70% of coarse grains (0.5–1.5 mm) and 10% of pure alumina (1–10 μm). After sintering

in muffle at 1350°C the material reached a final apparent density of 1.6 g/cm^3 (without pressing). From this composite, three specimens with dimensions 10 mm x 23 mm x 105 mm were cut for mechanical testing.

1.1.2. Results

In Valenza et.al.'s [3] study, samples were sintered in a dilatometer up to 1460°C with a linear temperature ramp of 10 °C/min in order to define the optimal temperature for the further isothermal sintering tests. The dilatometer curve shows the start of sintering at 1100°C, a quite steady state rate in the range 1200–1400°C, while from 1400°C the process has a sharp acceleration.

Then, for isothermal sintering, two temperatures have been chosen: 1300°C and 1400 °C; samples were kept at constant temperature for 2 h and then cooled. Relative shrinkage against time is sharply decreased in first 10 minutes is, then the decrease is slightly slow.

Ten cylindrical samples sintered in a muffle furnace at 1350°C were mechanically tested in diametral compression. A mean tensile strength of 20 MPa was obtained, comparable to that of a standard refractory. The Weibull curve shows a certain dispersion of data with a low value of the Weibull parameter *m*, as expected for this type of testing. In order to investigate the mechanical properties of the composite material made by fine powders and coarse grains, elastic modulus and flexural strength have been measured on the three specimens described in Section 1.1.1. The dynamic elastic modulus was evaluated by means of the resonance method resulting in a mean value of 18 GPa while the flexural strength, evaluated by 4-point bending test machine, gave a mean value of 9.9 MPa. All samples broke apart instantaneously after reaching the rupture load [3].

The dilatometric curves for isothermal sintering described in the previous section can be converted into semi-logarithmic plots of $\ln(d\rho/dt)$ vs. ρ, the relative density of the compact. These plots, typically, appear as descending straight lines in the initial/ intermediate stage of sintering and bend down in the final stage, when the sintering rate decreases, tending asymptotically to a final density ρ_f . The main features of the plots

are therefore ρ_f and the (negative) slope S of the linear part. The higher is S, the faster is the process.

At constant microstructure, i.e. in the absence of grain growth or particle rearrangement, this function is independent of both temperature and particle size. It follows that, starting from equal green compacts, the semi-logarithmic plots should have the same shape, being only translated along the vertical axis. In particular the slopes in the stationary part of the kinetics should be equal. The final parts of the curves could be different, however, if grain growth occurs.

In the case of the present experiments the final microstructures of the two compacts show that no grain growth had occurred. Yet, the two plots are very different in shape: the slopes in the linear parts are S = -91 for sintering at 1300°C and S = -21 for sintering at 1400°C, and the final densities are respectively 0.815 and 0.865. One can see that the lowest values of ρ correspond to the mechanism of viscous flow. Thus the higher S obtained for samples sintered at 1400°C can be explained with the activation of viscous flow in the silica phase of the molochite powders. The low value of S for the sample sintered at 1300°C is due to desintering phenomena, namely particle rearrangement followed by ruptures of already formed necks, as suggested also by the aspect of the final microstructure. Assuming the slope S as an index of the sinterability of a powder compact, it is worthwhile noticing that the sample of molochite powder from re-use of casting shells, when sintered at 1400°C, has a sinterability quite similar to that of alumina. A difference is, however, that the molochite powders seem to have some difficulty to reach a high final density. This point might be not so important in the present case, because the mechanical strength of the sintered powders is at all events sufficient when they are used as a fine aggregate in refractories. In the mechanical testing of samples obtained by sintering an aggregate of fine powders with coarse grains of the same material, the post-rupture behaviour deserves attention. In fact, this sample breaks apart instantaneously after reaching the rupture load when tested in bending.

Powders obtained from waste of ceramic casting investments are essentially molochite with a considerable fraction (53 wt%) of vitreous silica. Milled to a size of 1–10μm such powders have good sinterability at a temperature of at least 1400°C and can be proposed for use as a fine aggregate in refractory tiles [3].

The mechanical properties of sintered composites formed with a matrix of fine waste powders and an inert coarse phase of the same material are comparable with those of conventional mullite/alumina refractories. The choice of the coarse phase, however, is crucial to provide an adequate resistance to crack propagation, which is essential to resist thermal shocks .

Not much research was devoted to the sintering behavior of zircon-mullite mixture to produce zircon-toughened mullite [3].

Since mullite is a refractory which has a high sintering temperature, magnesia addition is necessary for sintering at low temperatures. The study below gives the effect of magnesia on sintering performance of zircon-mullite mixture at lower temperatures [18].

The sinterability of two industrial mullite powders, in the presence of MgO as a sintering aid, was investigated. A glassy phase, which was generated during preparation, was present in both powders; this glassy phase had a strong influence on sintering, depending on its content, composition, and spatial distribution. MgO promoted sintering in the presence of a liquid phase. Investigations allowed a better understanding of the influence of MgO and the glassy phase on the sintering behavior and the formation of new phases. Most of the phases, in fact, can be explained by using the $MgO–Al_2O_3–SiO_2$ phase diagram, even in such complex systems [18].

The critical feature of the mullite powders is their sinterability, which is strongly dependent on their composition, particle-size distribution, and impurity level. A pre-existing glassy phase that originates from the preparative path also is present in these powders. The strong influence of its content, composition, and spatial distribution has been shown. The purpose of this work is to understand the role of the composition of the glassy phase and MgO that is added as a sintering aid on the behavior of two commercial mullite powders during sintering. The formation of new phases in these two mullite powders also is studied.

Based on suggestions in the literature, MgO (purity of >99%, mean particle size of ~1μm after milling; Carlo Erba) was chosen as a sintering aid. Mullite–MgO

mixtures in the compositional range of 0–3 wt% MgO were prepared via an ultrasonic homogenization of alcoholic suspensions.

The green densities for mullite powders A and B, after uniaxial pressing, were 60% and 44% of the theoretical value, respectively. The higher green density of compact A can be attributed to its particle-size distribution-particularly, the presence of a large amount of fine particles that can fill the intergranular voids between the larger particles.

As investigating the dilatometric behavior (linear shrinkage and density) of the mullite powders, the two materials showed no relevant densification without MgO addition. Higher densification rates are associated with the materials that had MgO added to them.

XRD analyses on the pellets that were sintered at a temperature of 1550°C for 3h showed the appearance of secondary phases that were due to the presence of the sintering aid. Phase evolution during sintering also can be understood using the above mentioned phase diagram, Figure 1.1 [18].

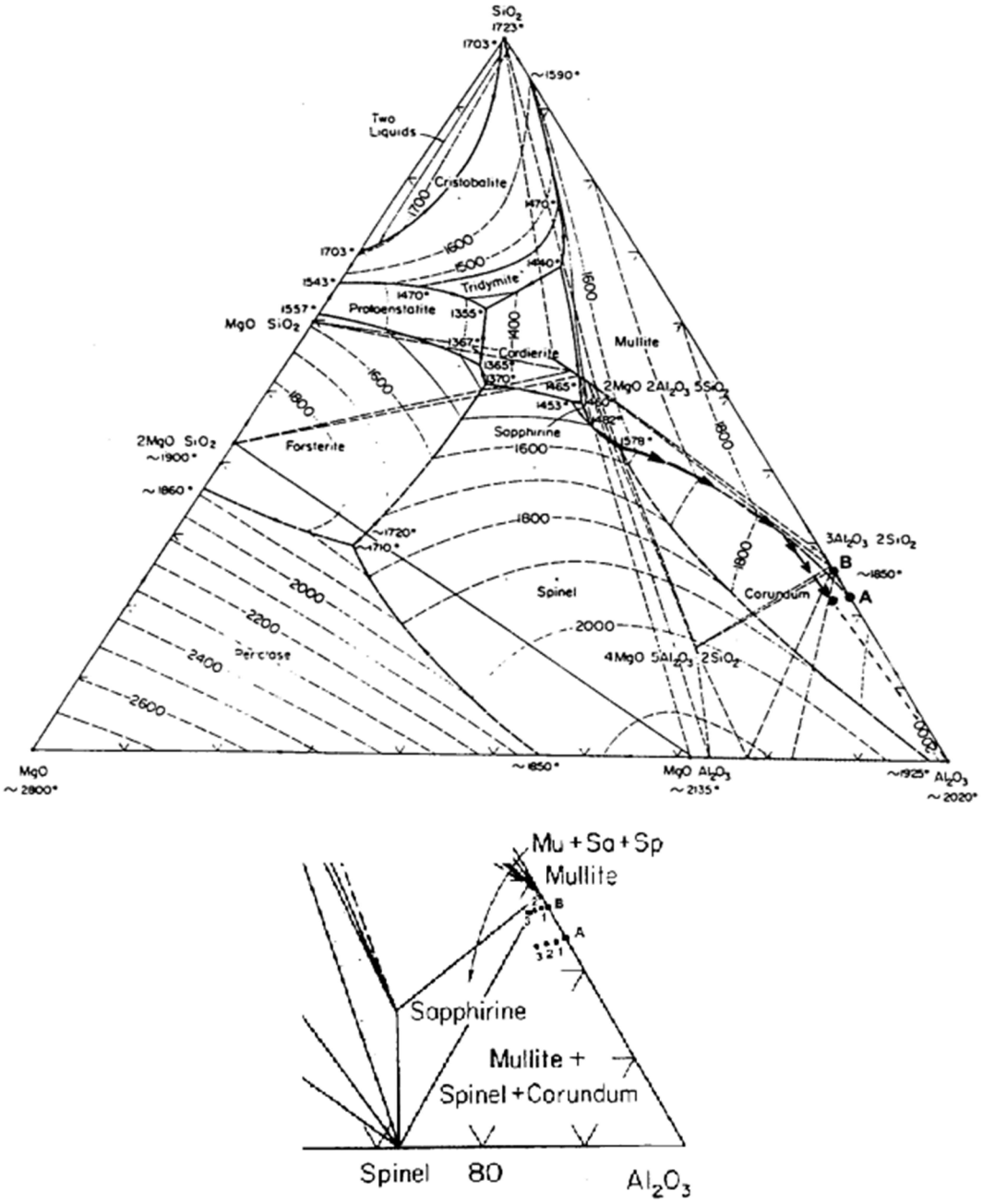


Figure 1.1- $MgO–Al_2O_3–SiO_2$ phase diagram. The smaller diagram at the bottom is an isothermal section of the diagram at 1460°C, showing the investigated composition with the addition of 1, 2, and 3 wt% of MgO. (From Schreyer and Schairer.17) [18]

Most illustrations are representative of average material microstructures; however, particular aspects of microstructural development also have been evidenced in some cases. The role of the sintering aid is difficult to show in the case of mullite powder A, because full sintering was not achieved, even when 2 wt% of MgO was

added. The broad particle-size distribution and the presence of hard agglomerates make it difficult to identify agglomerates that are formed during powder synthesis and the grains that are sintered during treatment at a temperature of 1550°C.

However, mullite powder A, with and without MgO, does show the following:

(1) Large and coherent diffraction domains (up to 10 μm) that probably developed during powder synthesis;

(2) Large pockets of glassy phase enclosed inside the hard agglomerates that probably were inactive during sintering;

(3) A portion of glassy phase that also was present at some grain boundaries, although microstructural observation could not identify whether it was already present before sintering;

(4) The presence of crystalline α-Al_2O_3 in the glassy pockets after sintering;

(5) EDS microanalysis that consisted of randomly focusing the 40-nm-spot-size probe beam on a succession of approximately twenty grains in different specimen zones detected changes in the composition of the mullite grains. These compositions changed considerably from one grain to another. The amount of alumina was in the range of 68.3– 87.1 wt%; sometimes, very high local alumina amounts were detected, which supports the hypothesis of free α-Al_2O_3 in the mullite grains. The mean alumina concentration of 76.5% is very close to the value that was obtained via chemical analysis after sintering (76.75%); and

(6) Grain contours that appear to be rounded after sintering.

Mullite powder B without MgO contained hard agglomerates, mostly isolated grains with an occasional agglomeration of small crystallites. The mean grain size was a few micrometers but was 100 –200 nm for the small crystallites. The glassy phase was generally well-distributed around the well-developed faceted grains. Thus, sintering was promoted by the grain linkage that was due to a well-distributed glassy phase [18].

Microanalysis showed that the composition of mullite powder B is quite constant. The alumina content is in the range of 70.4 –76.8 wt%, with a mean value of ~74 wt%, which is close to the value that has been obtained via chemical analysis (73.23%). This slight shift toward an alumina-richer composition is consistent with the

previous statements, which also located mullite powder B materials in the mullite+spinel+α-Al_2O_3 stability field.

Mullite powder B with 1 wt% of MgO added after sintering showed considerable grain growth. Many crystallites showed an elongated shape with regular faceted boundaries. Systematic electron diffraction indicated that most of these boundaries were of the {110} type, relative to the greatest apparent surface. The mullite grains exhibited an elongated shape.

The glassy phase was still present and well distributed at the grain boundaries. Triple-point junctions that were filled with glassy pockets also were observed.

When the corresponding unquenched material is considered, EDS measurements of the composition of some glassy-phase pockets show a smaller MgO amount in the glassy phase (~5 wt%). Partial glassy-phase recrystallization occurs and spinel appears during slow cooling. Significant growth of many mullite grains and the presence of well-faceted grains boundaries parallel to the low-energy mullite planes also are observed after sintering [18].

Based on these results, the following mechanism can be suggested to occur during sintering. MgO additions enhance the amount of glassy phase and induce partial mullite dissolution. This dissolution mainly involves the high-energy surfaces (which are less stable) of the mullite grains. Thus, the morphology of the rounded mullite grains changes to low-energy well-faceted grains. Furthermore, during cooling, a partial crystallization of the glassy phase can lead to a significant grain growth of mullite, extending the faceting phenomenon. The mechanism of this process is not well-known, and the composition, the amount of the glassy phase, and the thermodynamic stability of the different phases are observed to have a strong influence.

The SiO_2:Al_2O_3 ratio in the glassy phase at the sintering temperature (which is 2.5, as evaluated on quenched sample B with 1 wt% of MgO added) is significantly greater than that in the crystalline mullite, but also is higher than that in the initial glassy phase of the as-received material (~1.7). Therefore, the glassy phase partially dissolves the mullite.

The crystallization of spinel grains induces modification of the surrounding glassy-phase composition during slow cooling. Spinel, α-Al_2O_3, and mullite appear, and most of the spinel crystals are entrapped in the mullite grains during devitrification of the liquid phase, probably because of low interfacial mullite/spinel energy. Conversely, α-Al_2O_3 grains exist in equilibrium with mullite and liquid in the quenched materials, according to the equilibrium diagram, as observed via TEM [18].

This research represents a preliminary approach to microstructural evolution and the formation of new phases in the complex system of commercial mullite powders during sintering. The following conclusions can be drawn:

(1) The composition, amount, and spatial distribution of the glassy phase, which is always present in industrial mullite powders, significantly influence the sinterability of the powders.

(2) MgO addition promotes sintering in the presence of a liquid phase.

(3) The formation of this MgO-containing liquid at the sintering temperature induces mullite dissolution, which mainly involves the high-energy surfaces of the mullite grains and induces the appearance of low-energy, well-faceted grain boundaries.

(4) Mg-Al spinel crystals form as a result of devitrification of the liquid phase during slow cooling. The mullite grains can grow during devitrification, entrapping the spinel precipitates.

(5) The formation of additional phases is inhibited during quenching, and only mullite and α-Al_2O_3 can be observed [18].

The aim of this work is to recycle investment casting mould wastes that can not be used for casting more than once. By this way, this investigation will be carried out to produce value- added materials in ceramic industry in order to reduce the production cost and as well as reduce the environmental pollution.

2. MATERIAL AND METHOD

Based on the information present in literature, the study on the recycling of investment casting shell powders was completed and described below.

2.1. Sample Preparation

Investment casting shell moulds were supplied from Gedik Casting & Valve Ltd., Pendik/ISTANBUL. Both used and unused pieces of the moulds are shown in Figure 2.1. These samples were crushed into small pieces by a jaw crusher and then ground by Fritsch Vibrating Cup Mill to obtain required fine powder. The powders were sieved by Fritsch Analysette sieve set (63µm, 45µm and 25µm sieves) and the powders with particle size below 63µm were used in the experiments.



Figure 2.1- Unused (left) and used (right) pieces of the investment casting shell moulds

In order to determine composition and mineralogical phase differences between two samples, chemical composition of unfired and fired samples were determined by XRF (Rigaku RIX 2000). Minerological analysis of as received unused and used shell powders samples after sintering was performed by XRD (Rigaku Rint 2200).

Thermal behavior of the powders were analysed by thermogravimetry-differential scanning calorimetry (TG/DSC) instruments (Netzsch STA409 CD) in flowing air atmosphere at a heating rate of 10K/min. up to 1490°C which was the maximum limit of the test equipment.

Microstructural analysis were performed by optical microscopy (Nikon Eclipse L150) and SEM (Jeol JSM 6360). EDS analysis (ThermoNoran SystemSix) was also carried out and after SEM examination and SEM photos were also taken.

2.2. Sample Preparation for Sintering

Samples for sintering were prepared in different compositions to observe the sinterability of the powder and the effect of sintering aid addition on sintering and densification development, and also to determine the optimum temperature of sintering for better densification. As a sintering aid, -25µm MgO powder, which was supplied from Kümas Manyezit Sanayii A.S.-Kutahya, was used to promote sintering. Other additives such as hexamine and ethyl alcohol were also used as binder and plasticizer, respectively, for sample compaction. In literature, MgO is found useful to decrease the sintering temperature in mullite containing ceramics and also preventing the glassy phase formation that causes a decrease in compression strength [18].

These samples were prepared in 4 different compositions. Table 2.1 shows the compositions of the samples.

Table 2.1 Compositions of samples

Sample Type	Sample Composition(wt%)			
	Used Mould Powder	**MgO**	**Hexamine**	**Ethyl Alcohol**
No MgO added sample	4.75 g	-	0.25 g	3-5 drops
1% MgO added sample	4.70 g	0.05 g	0.25 g	3-5 drops
2% MgO added sample	4.65 g	0.10 g	0.25 g	3-5 drops
3% MgO added sample	4.60 g	0.15 g	0.25 g	3-5 drops

Each sample was prepared by mechanical mixing of weighed mould powder, MgO powder and hexamine powder homogeneously. Then as a binder ethyl alcohol was added and mixed well to prevent lamination. Each 5 g sample mixture was pelletized in a hardened steel die under 2500 psi pressure by uniaxial pressing device. Clindirical pressed pellet nominal dimensions were 25 mm in diameter and 6.4 mm in height.

3 sets of samples (each set contains 4 different composition samples) were prepared for sintering. Sample sets were sintered to 1450°C, 1475°C and 1500°C

respectively using Nabertherm (HT 40/18) electrically heated sintering furnace. In Table 2.2, sintering programs for 3 sintering temperatures are presented.

Table 2.2- Sintering program for 1450°C, 1475°C and 1500°C

Sintering program	
Temperature	**Heating/cooling rate**
40°C - 300°C	6°C/min
300°C - 300°C	1 hour hold
300°C – 1450/1475/1500°C	8°C/min
1450/1475/1500°C - 1450/1475/1500°C	3 hours hold
1450/1475/1500°C - 40°C	5°C/min

Each sample set was loaded into the furnace and the suitable sintering program was applied and then sintering was carried out.

The sintered samples were assigned a number according to composition and sintering temperature and will be called with the numbers given in Table 2.3.

Table 2.3 Sintered sample names

Sample name	**Sample type**
1	1450°C - no MgO
2	1450°C - 1% MgO
3	1450°C - 2% MgO
4	1450°C - 3% MgO
5	1475°C - no MgO
6	1475°C - 1% MgO
7	1475°C - 2% MgO
8	1475°C - 3% MgO
9	1500°C - no MgO
10	1500°C - 1% MgO
11	1500°C - 2% MgO
12	1500°C - 3% MgO

Shrinkage, bulk density, apparent porosity and water absorption were measured by the help of a caliper (Mitutoyo) and a digital scale (Mettler Toledo AB104-S) at room temperature. Hardness measurement of each sample was performed using Future-Tech Fully-Automatic Microhardness Testing System (FM-ARS7000) room temperature under 200 gf load applied for 15 seconds (dwelling time).

3. RESULTS AND DISCUSSION

3.1 . Experimental Results

3.1.1. XRF and XRD analysis of shell powders

XRF results of both of the samples are given in Table 3.1. XRF analysis show that there is no significant difference in oxide compositions between two samples. The most abundant oxides are Al_2O_3, SiO_2, K_2O, Fe_2O_3 and ZrO_2. By the help of XRD analysis phases determined in each sample. XRD analysis results were presented in Figure 3.1 Figure 3.2 and Table 3.2. Unused powder contains mullite ($Al_6Si_2O_{13}$), zircon ($ZrSiO_4$) and crystoballite (SiO_2) phases, whereas used powder contains mullite ($Al_6Si_2O_{13}$), zircon ($ZrSiO_4$) and tridymite (SiO_2) phases.

Table 3.1- Compositions of unused and used shell powders by XRF

Oxide	Unused Shell Powder Composition (wt%)	Used Shell Powder Composition (wt%)
Al_2O_3	31.1	32.7
SiO_2	50.5	51.5
K_2O	2.47	2.02
Fe_2O_3	1.54	1.84
ZrO_2	12.9	10.2
Other oxides	1.49	1.74

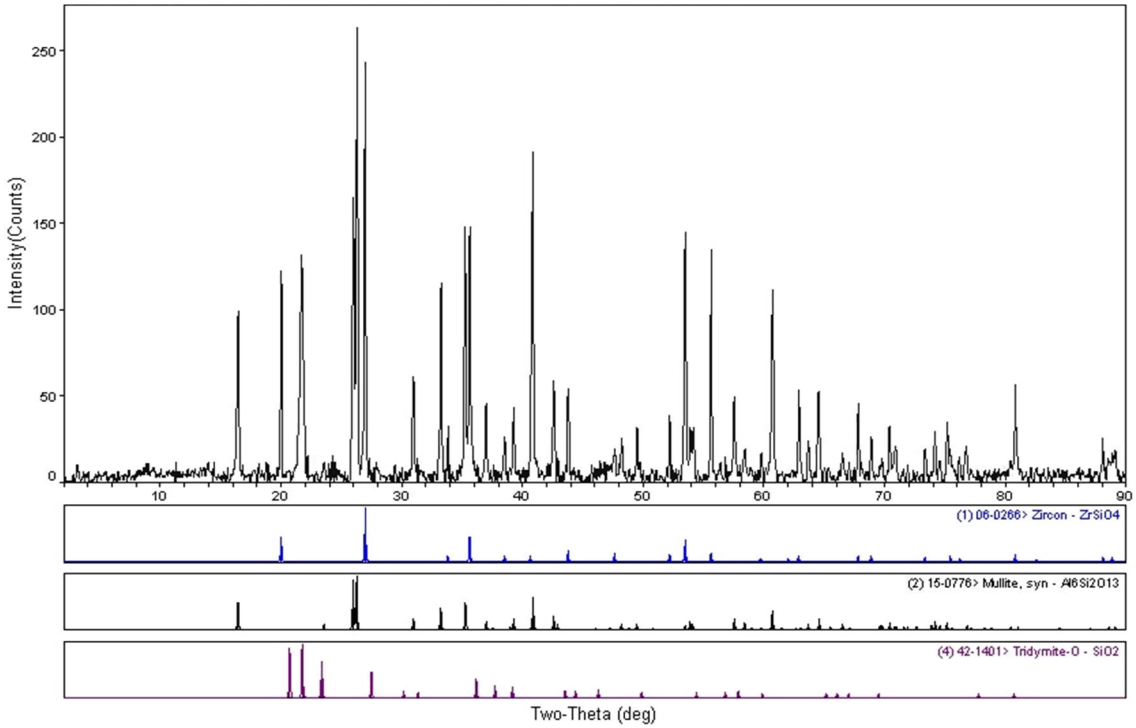


Figure 3.1- XRD analysis pattern of unused shell powder

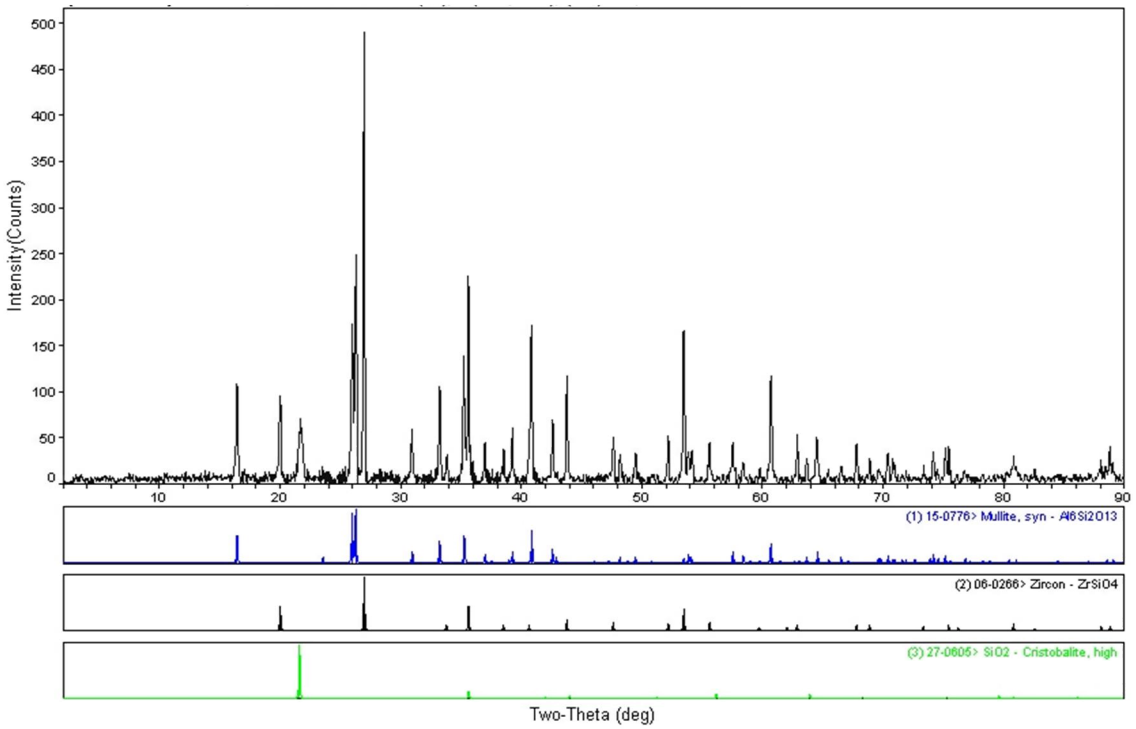


Figure 3.2- XRD analysis pattern of used shell powder

Table 3.2- Phases detected by XRD analysis of used and unused mould sand

Sample Type	Phases detected
Unused mould sand	Mullite (Al6Si2O13), zircon (ZrSiO4), tridymite (SiO2)
Used mould sand	Mullite (Al6Si2O13), zircon (ZrSiO4), crystoballite (SiO2)

3.1.2 Thermal behaviour analysis

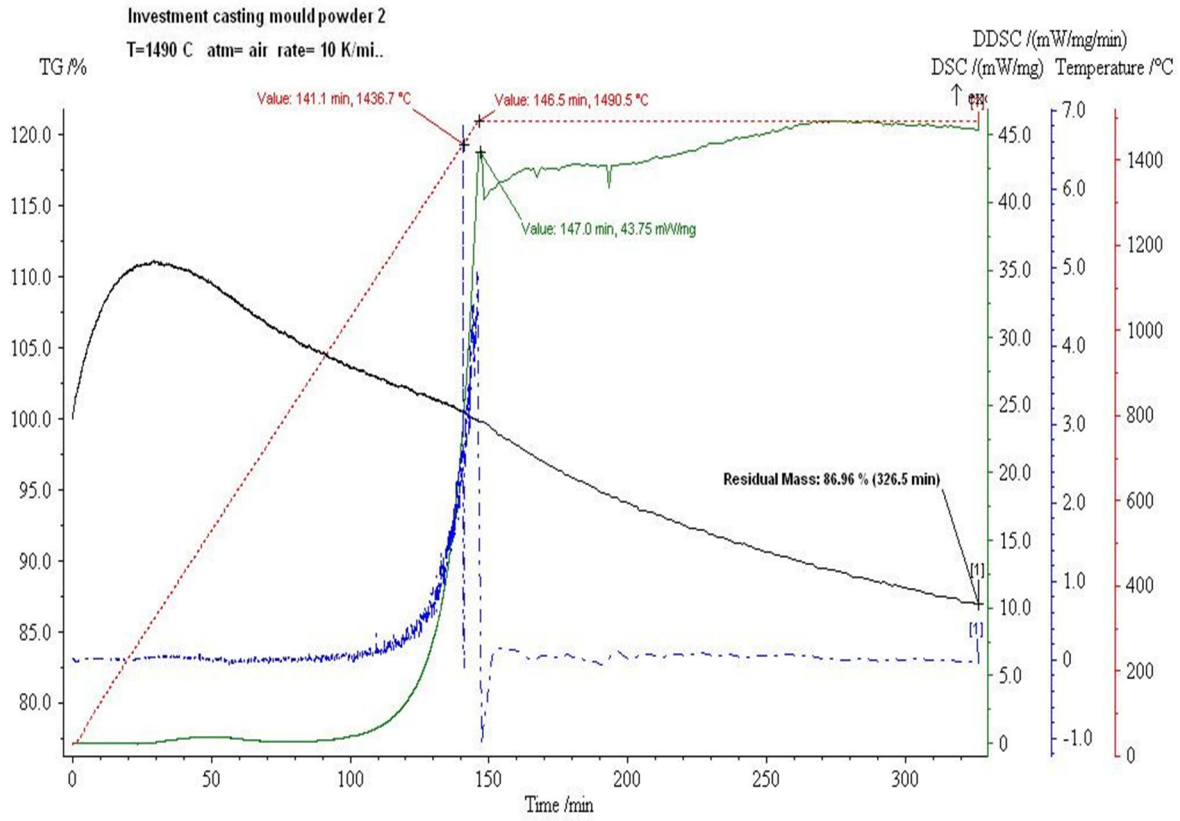


Figure 3.3- TG/DSC analysis graph of unused shell powder

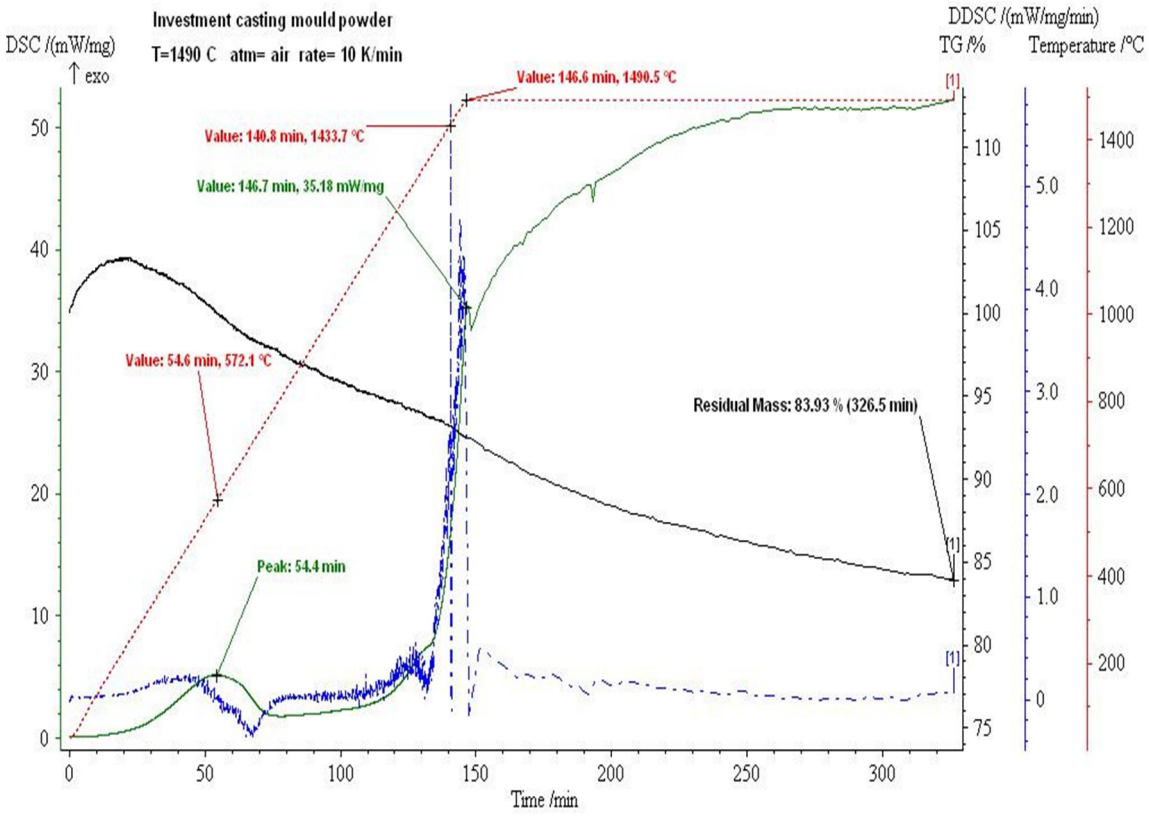


Figure 3.4- TG/DSC analysis graph of used shell powder

TG/DSC curves of the as received and used cast shell powder shown in Figure 3.3 and Figure 3.4 respectively, TG curve of the sample showed weight loss of 16% at 1490°C. Weight loss appeared to be continuous with increasing temperatures during the test. Weight loss could be attributed to firstly moisture absorbed during sample grinding, and secondly residual carbon from burnt wax, which was the main material of the pattern used for mould formation. DSC curve of the sample exhibited two exothermic peaks at about 572°C and 1433°C. The first exothermic peak is assigned to burning of residual carbon coming from wax pattern, and the second one is an intense and sharp peak which may be attributed to the reaction between mullite and zircon sand.

3.1.3. Microstructural evaluation

According to SEM photos, the morphology of the used mold powder can be seen in Figure 3.5, revealing angular shape particles. The grain size distribution was in the range of 1µm-25µm which was in good agreement with required grain size distribution.

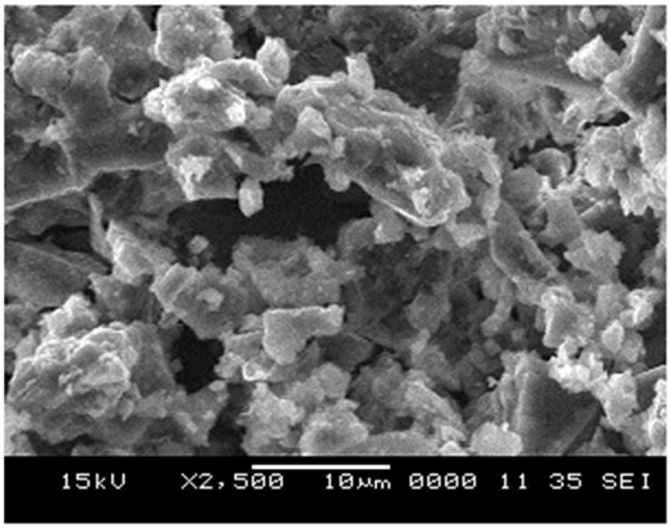


Figure 3.5- SEM micrograph of used mold powder after milling and sieving

At the end of the sintering process of the samples, they were taken out of the furnace, the top macrostructural view of the samples are shown below in Figure 3.6.

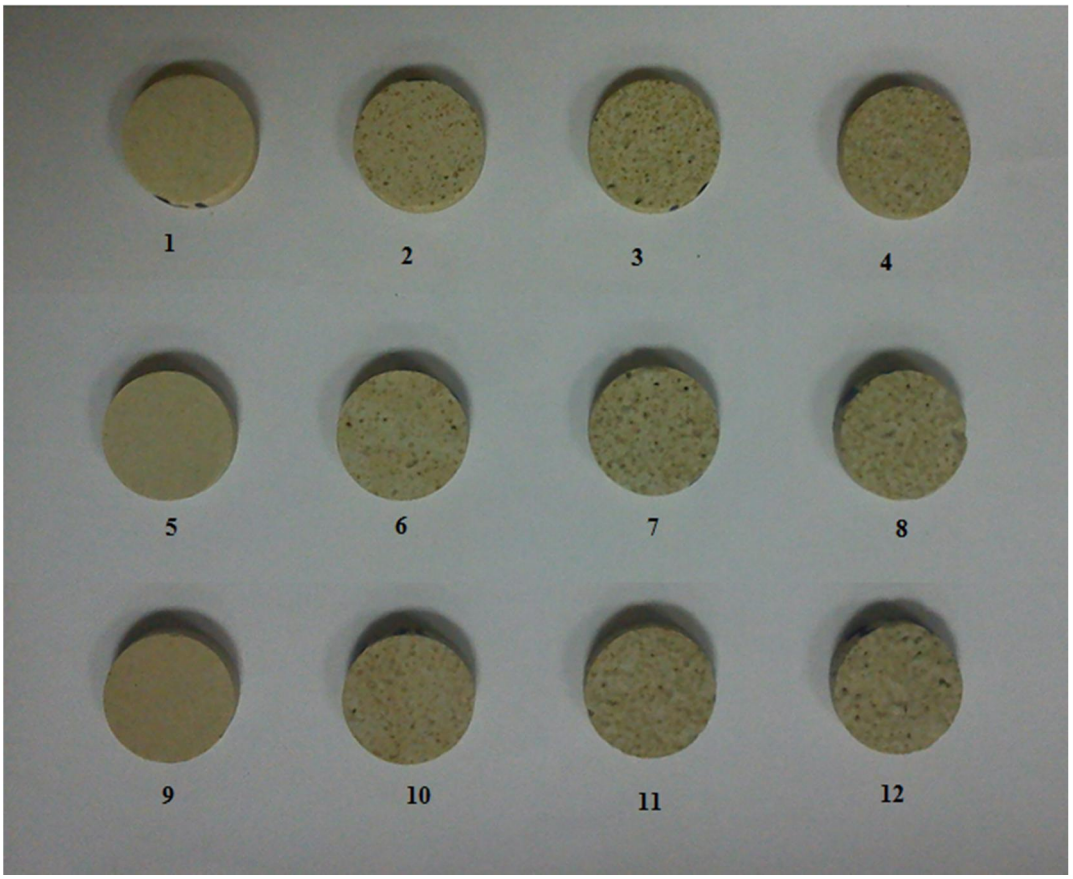


Figure 3.6- Top view of the sintered samples

According to the observations of macrostructural evaluation, color of sintered samples appeared to be light yellow with no MgO additon samples and getting darker as MgO addition increases from 0 to 3 wt %.

The samples were examined under optical microscope – Nikon ECLIPSE L150 (Nikon coolpix 4mp digicam attached). The photos of sample 3 at x150, x300, x600 magnifications are given below (Figure 3.7).

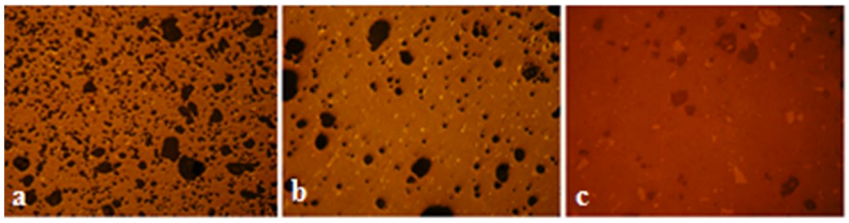


Figure 3.7- Optical microstructure photos of 2% MgO added sample , sintered at 1450°C at x150, x300, x600 magnifications, respectively (sample 3)

SEM photos of the sintered samples in Figures 3.8 and 3.9. SEM pictures reveal that; in the matrix mullite needles were clearly identified whereas zircon sand ($ZrSiO_4$) reinforcing particles were found to be distributed randomly in the matrix. In Fig. 3.9, mullite morphology was identified in two forms; as needle and particles. Pores can also be seen in the matrix as larger in dimension because of the fact that sintering temperature, time or insufficient sintering.

MgO particles were used as sintering promoters. MgO addition into mullite matrix was proposed by several researchers as fluxing agent in mullite sintering [16]. No trace of reaction was found between zircon sand particles and MgO after sintering. SEM and EDS analysis revealed that MgO particles dissolved in mullite matrix forming a solid solution. It was also evident that MgO was present according to EDS analysis.

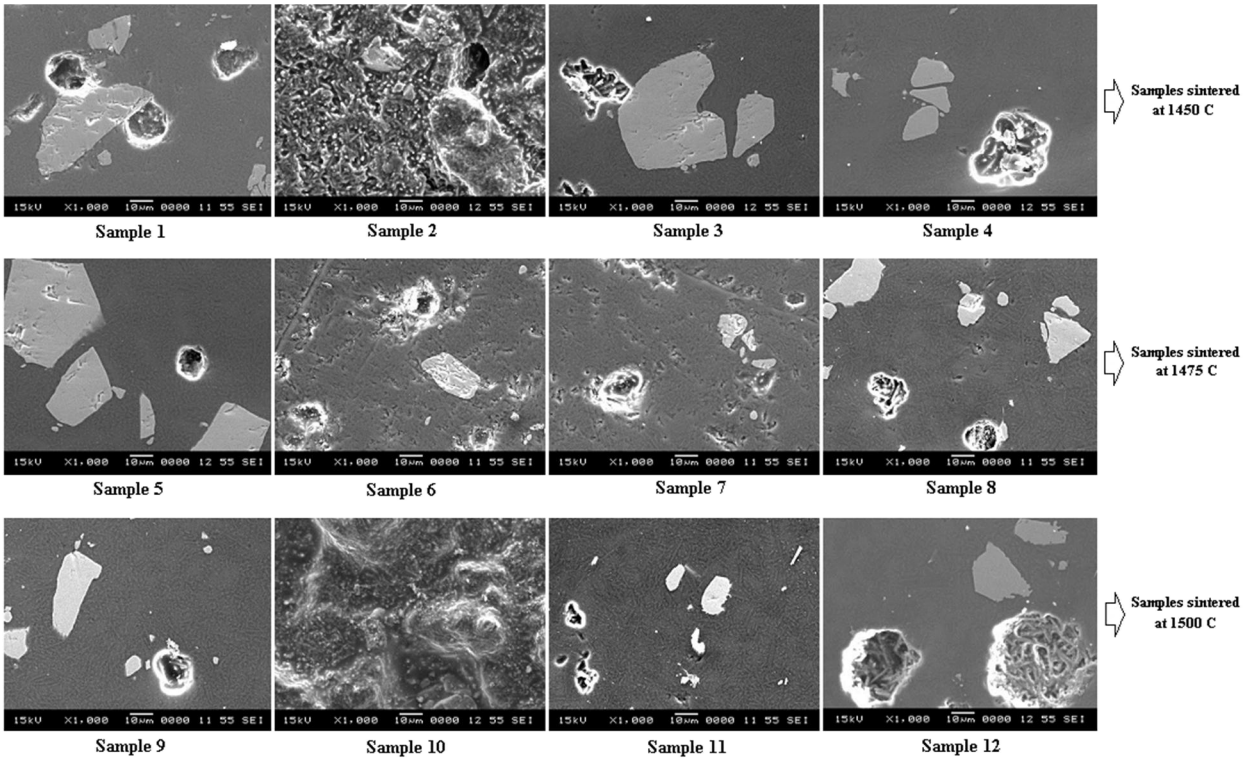


Figure 3.8- SEM photos of the sintered samples at 1450°C, 1475°C and 1500°C

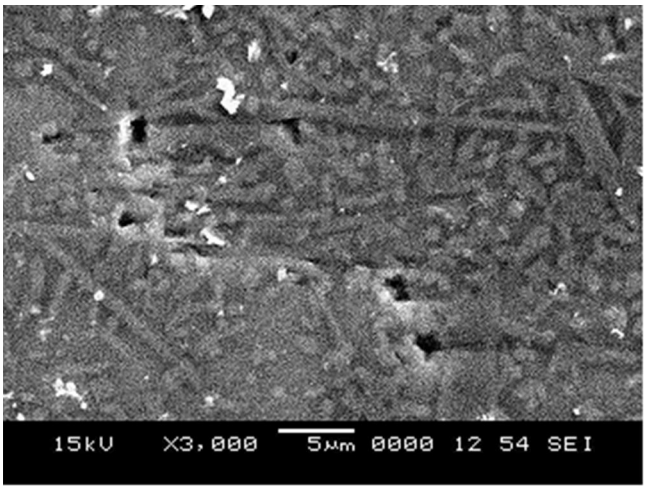
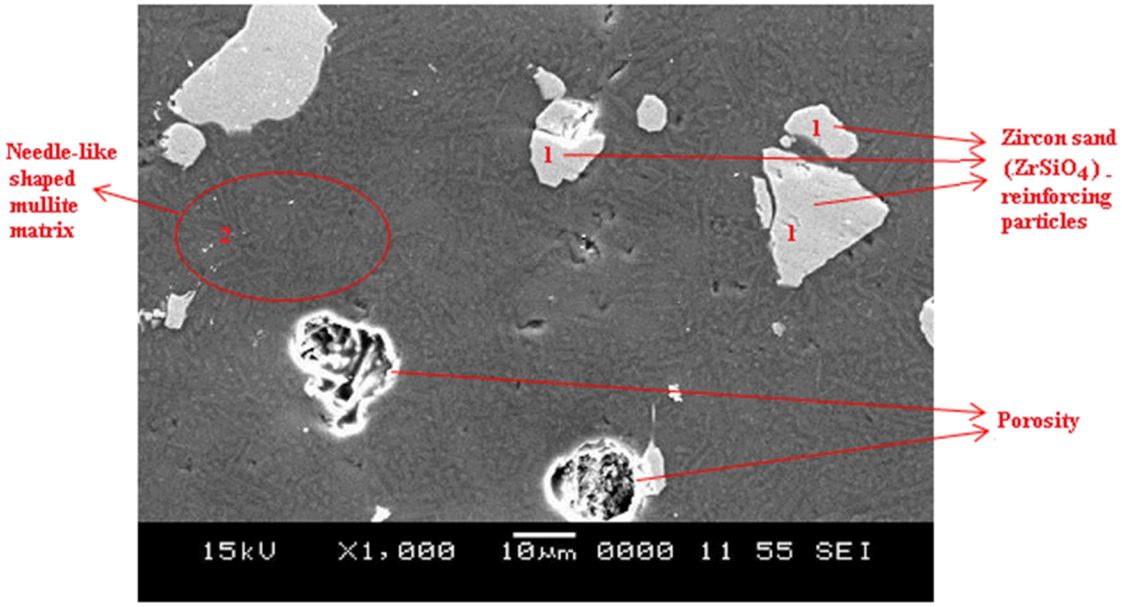


Figure 3.9- SEM micrograph of 2% MgO containing sample sintered at 1500°C (sample 11)

The phases observed and identified by the SEM photos and the phase compositions of the matrix and reinforcing particles detected by EDS analysis. The light gray and angular-shaped particles randomly oriented in the matrix are zircon sand particles with a composition given by Point 1, dark gray and needle like shaped matrix

forming a solid solution with MgO is mullite with a composition given by Point 2, in the Figure 3.10.



	MgO	Al2O3	SiO2	K2O	Fe2O3	ZrO2
EDS analysis_pt1		3.27	32.22			64.51
EDS analysis_pt2	1.39	38.31	56.29	1.22	1.67	1.12

Figure 3.10- EDS analysis of 3% MgO containing sample sintered at 1475°C (sample8)

3.1.4. XRD analysis of samples after firing

XRD analysis of all samples after sintering (Fig. 3.11-3.14) show that two phases are present; mullite and zircon. This is due to the fact that, starting raw materials contain Al_2O_3 and SiO_2, therefore after heat treatment during casting and sintering, these two oxides formed mullite. Zircon did not undergo any apparent phase transformation and remained as before.

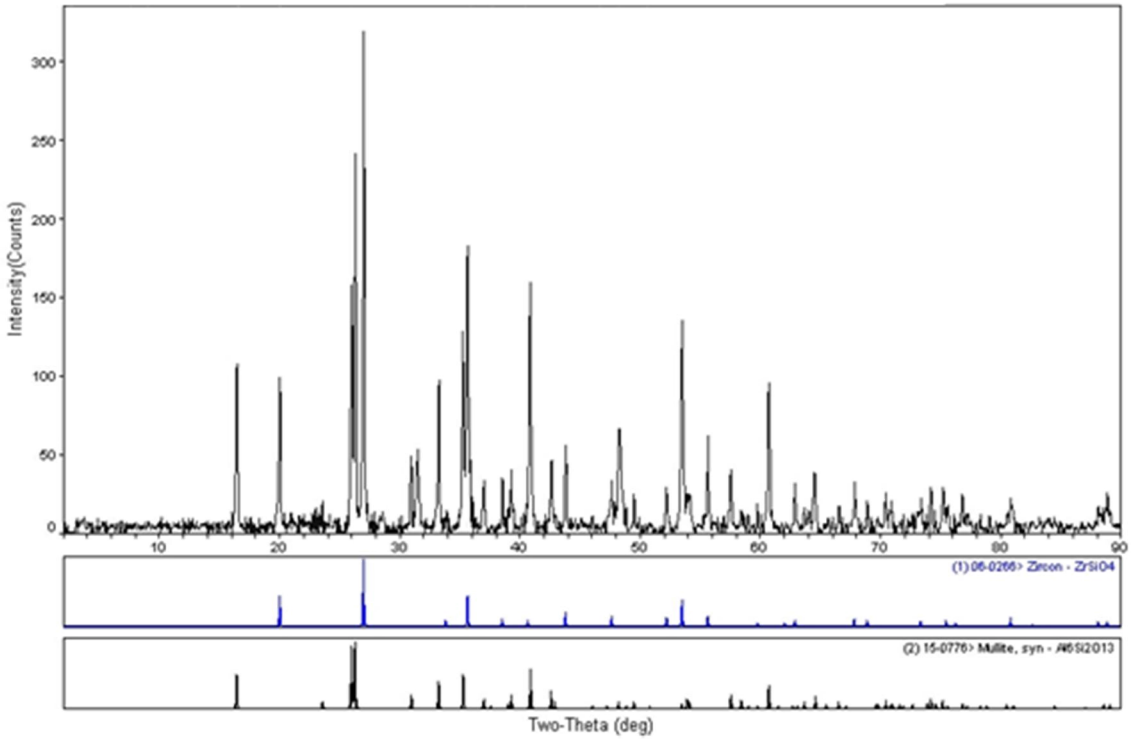


Figure 3.11- XRD analysis pattern of no MgO added sample at 1450°C

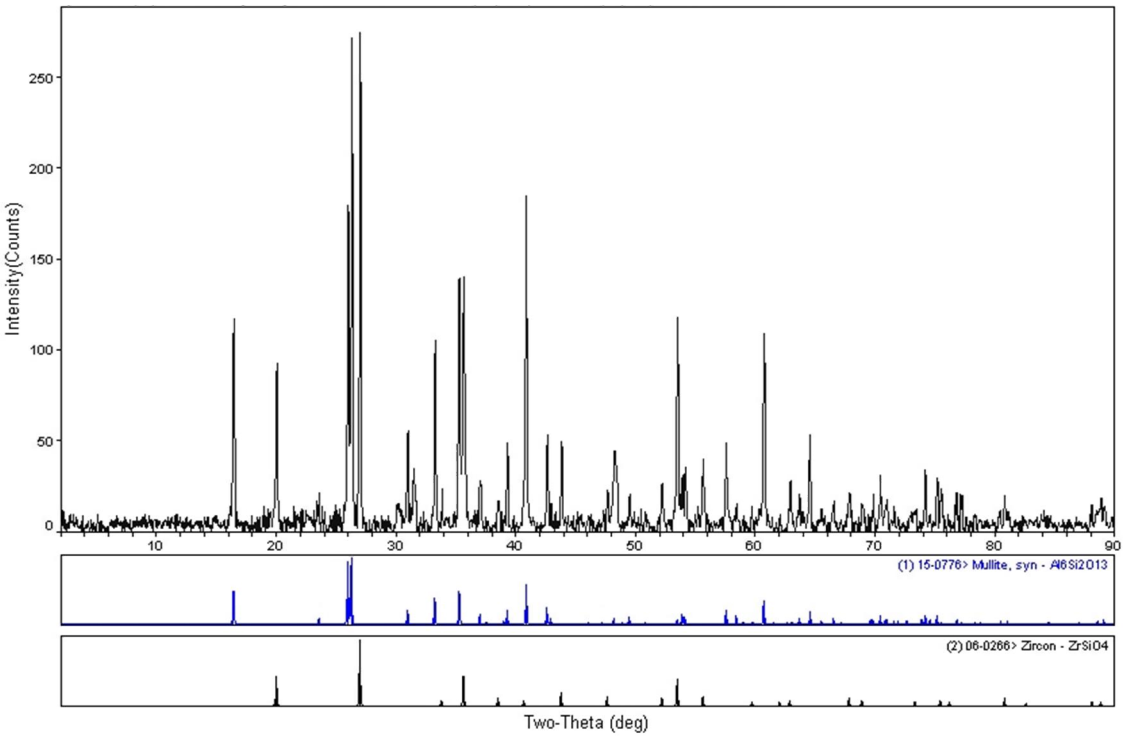


Figure 3.12- XRD analysis pattern of no MgO added sample at 1500°C

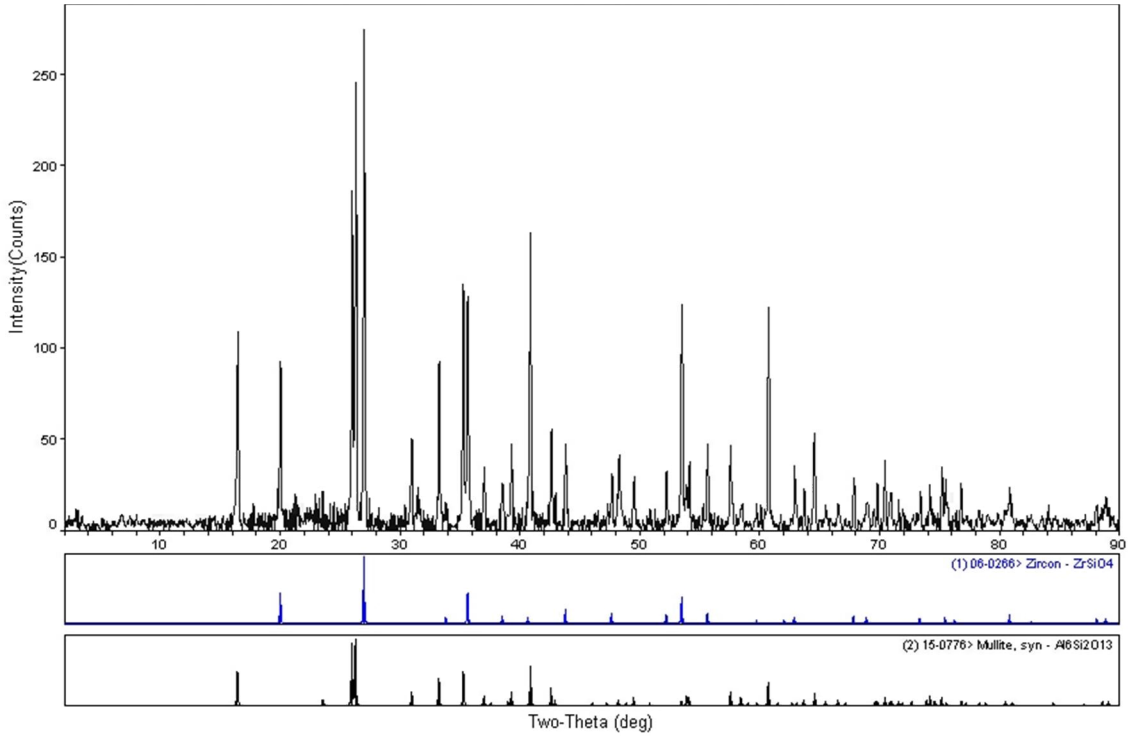


Figure 3.13- XRD analysis pattern of %3 MgO added sample at 1450°C

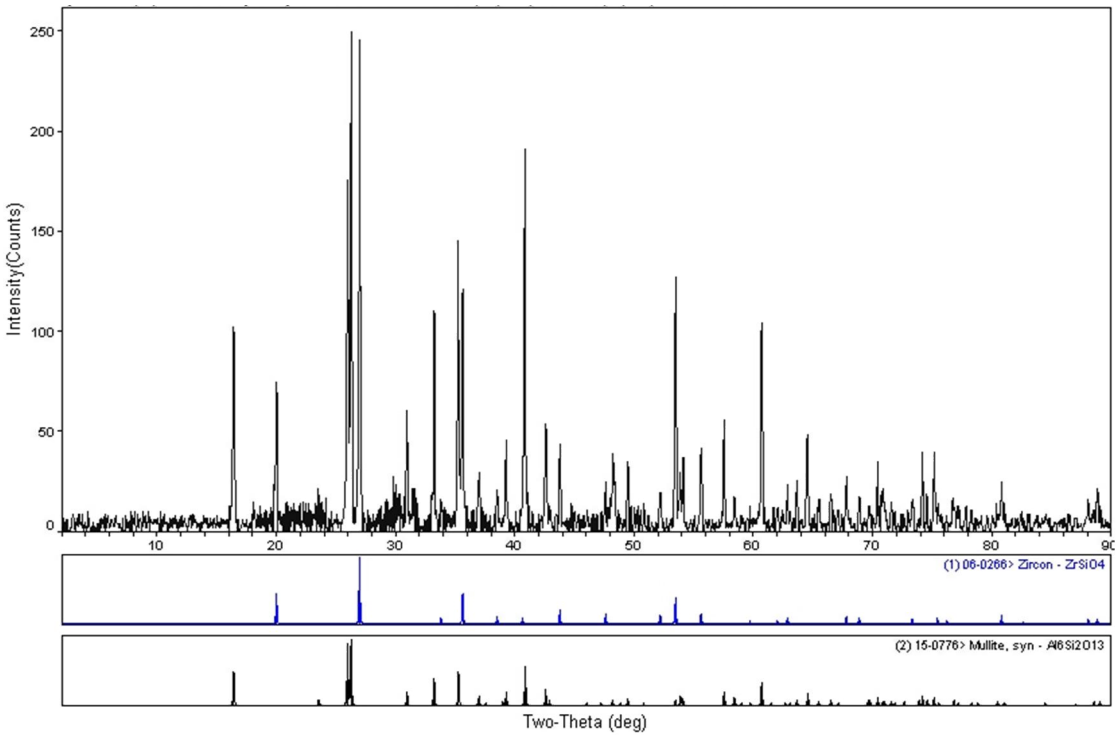


Figure 3.14- XRD analysis pattern of %3 MgO added sample at 1500°C

3.1.5. Some physical properties of samples after firing

To investigate the physical properties of the sintered samples, bulk density, apparent porosity, weight loss, shrinkage rate and water absorption tests were performed for all samples. Figure 3.15 shows that as the sinterability of mullite increases with the aid of MgO bulk density increases. This leads to densification of the microstructure by MgO addition. At increasing temperatures, the sample with same composition becomes more denser. As the bulk density increases with MgO addition, apparent porosity decreases (Figure 3.16), thus leading to decrease in water absorption (Figure 3.17). In Figure 3.18, at 1450°C, weight loss of the no MgO added sample is 6.54%, as the temperature reaches to 1475°C and 1500°C, weight loss of the sample reaches to 6.66% and 6.94%, respectively. Shrinkage, which is an indication of sinterability and densification, raise is also shown in Figure 3.19 due to temperature increase and MgO addition amount which suggest that sinterability of the sample is improving.

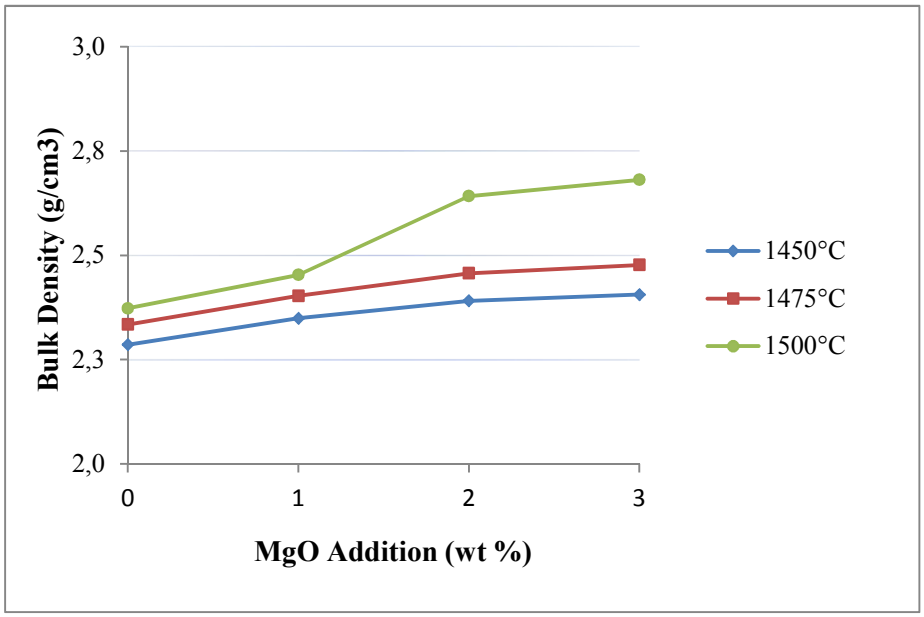


Figure 3.15- Bulk density variation as a function of MgO addition after sintering at 1450, 1475 and 1500°C for 3 hours

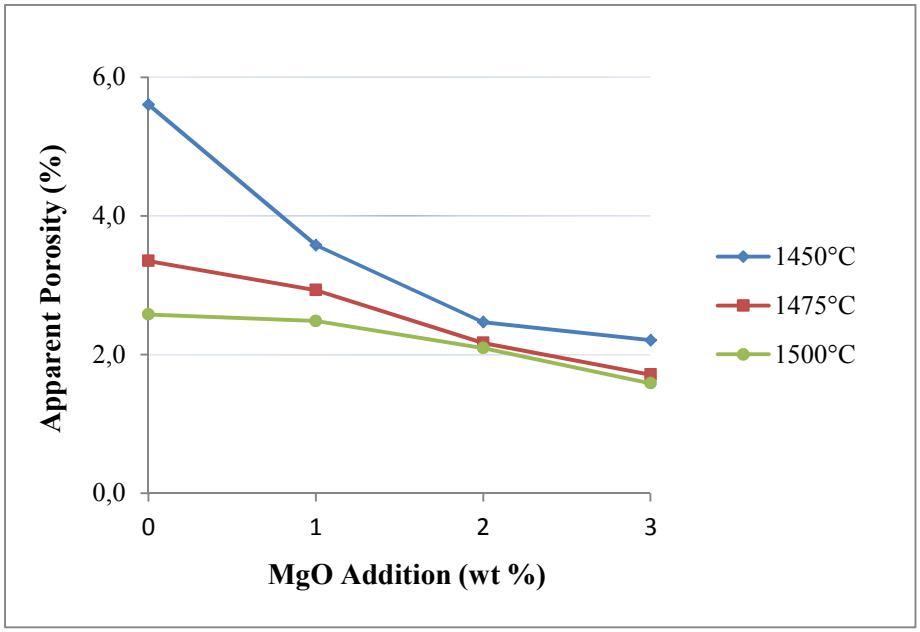


Figure 3.16- Apparent porosity variation as a function of MgO addition after sintering at 1450, 1475 and 1500°C for 3 hours

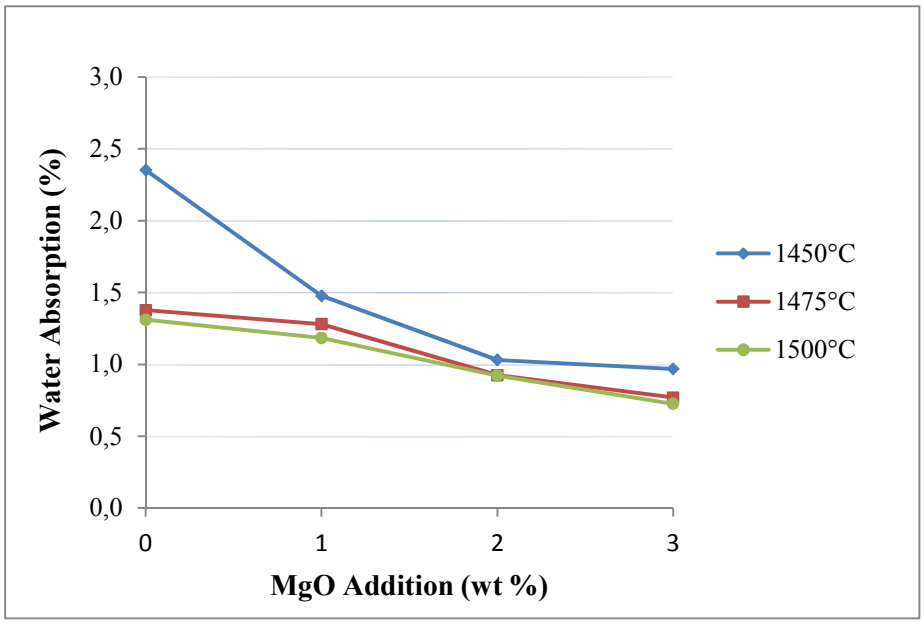


Figure 3.17- Water absorption variation as a function of MgO addition after sintering at 1450, 1475 and 1500°C for 3 hours

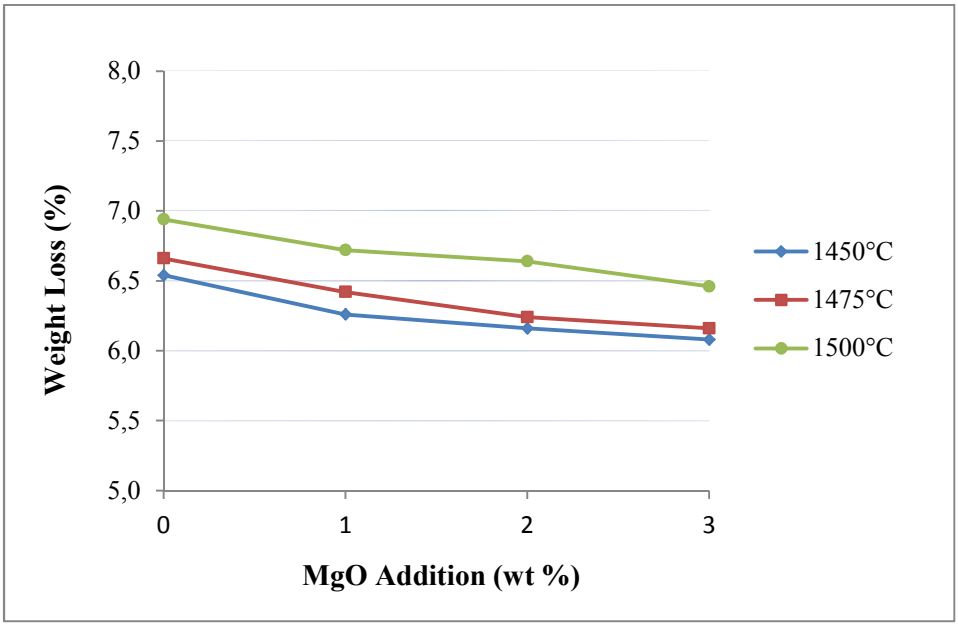


Figure 3.18- Weight loss variation as a function of MgO addition after sintering at 1450, 1475 and 1500°C for 3 hours

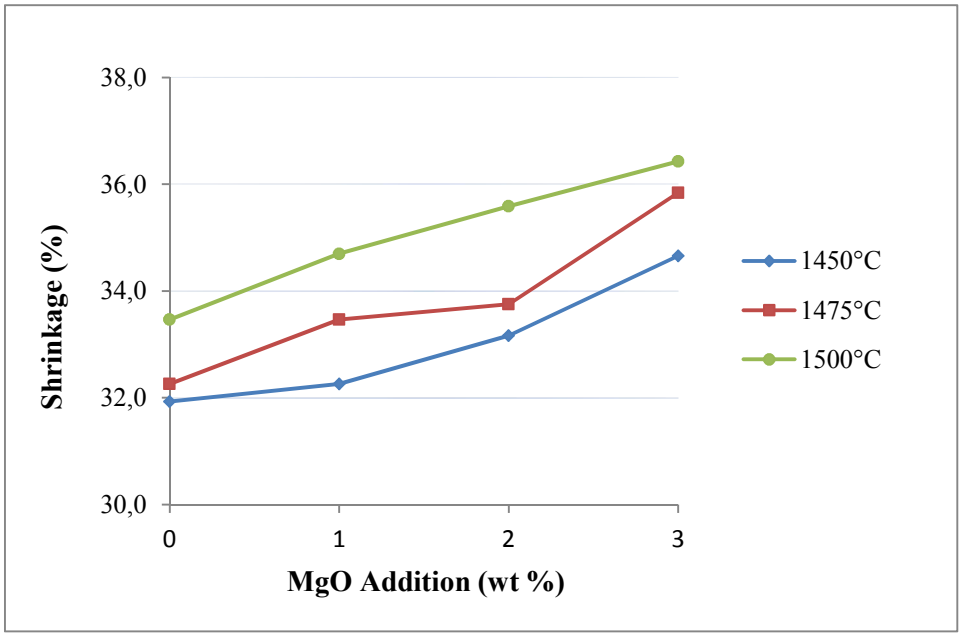


Figure 3.19- Shrinkage variation as a function of MgO addition after sintering at 1450, 1475 and 1500°C for 3 hours

As presented in Figure 3.18, weight loss of the samples slighly increased with the increase in sintering temperature whereas decreases with rising MgO addition.

Weight loss increment with rising sintering temperature can be attributed to evaporation of binder and plasticizer during sintering which resulted in weight loss.

3.1.6. Hardness of samples after sintering

Hardness were measured to evaluate the effect of sintering temperature and MgO addition on the mechanical properties. As presented in Fig. 3.20 hardness values rise with sintering temperature and sintering temperature increment. This result is a good agreement with Ouali et al [16]. Ouali et al [16] reported that the increase of MgO content in mullite from 0 to 3 wt % increased the hardness at 1600°C. As the hardness values were measured for the same composition samples at 1450,1475 and 1500°C, the same correlation is valid in Figure 3.20.

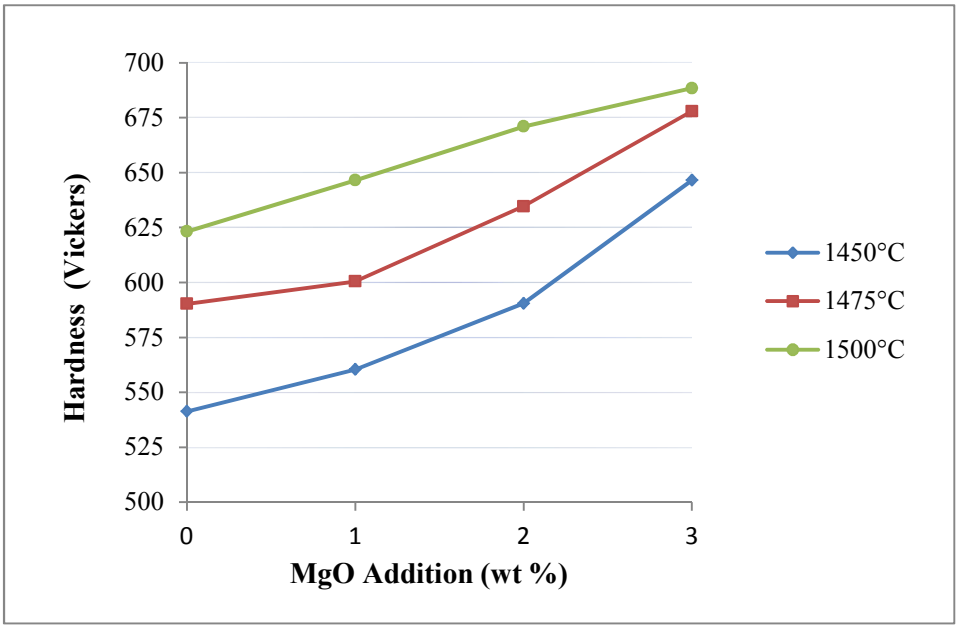


Figure 3.20- Hardness variation as a function of MgO addition after sintering at 1450, 1475 and 1500°C for 3 hours

4. CONCLUSION

Although investment castings are not as widely used as sand castings, they also produce solid waste, as they are usually destroyed when removed from a work piece. Spent mould sands are non-hazardous unless heavy metal alloy constituents are present. Spent wax, used as patterns for the molds, also contribute to solid waste. The patterns are removed by melting the wax and can usually be reused. Since investment casting waste casting shell mould sands can be used only once, it was decided to study on the recyling or beneficial reuse of waste casting shell mould sands which potentially poses ceramic raw material in their formulation such as mullite, quartz and zircon.

In this study recycling of mould sand was investigated. MgO addition was attempted between 0-3 wt % for densification. The compacted powder mixtures were sintered at the different sintering times at 1450, 1475 and 1500 °C for 3 hours. Following conclusions can be drawn from this study.

- As the sinterability of mullite increased with the aid of MgO, shrinkage of the samples increased, thus bulk density increased.
- The shrinkage rate increased with increasing magnesia addition at all temperatures, leading to decreasing apparent porosity.
- Bulk density increase with increasing magnesia addition at all temperatures caused to decrease water absorption.

As a final remark, MgO addition into mould sand can provide improved or better mechanical properties and reduces the sintering temperature for cost effective processing and recycling of the mould sand. MgO added investment casting waste mould sand can be partially used in some refractory applications for reinforcement purposes where operation temperature should be lower than 1500 °C.

REFERENCES

[1] http://www.custompartnet.com/wu/investment-casting

[2] http://en.wikipedia.org/wiki/Investment_casting

[3] Valenza, F., Botter, R., Cirillo, P., Barberis, F., di Foggia, M., Sottile, D. (2009), "Sintering of Waste of Superalloy Casting Investment Shells as a Fine Aggregate for Refractory Tiles", Ceramics International

[4] Mergen, A., Aslanoglu, Z. (2002), "Low-temperature fabrication of anorthite ceramics from kaolinite and calcium carbonate with boron oxide addition", Ceramics International, 29, 667–670

[5] Duran, C., Tur, Y.K. (2004), "Templated grain growth of textured mullite/zirconia composites", Materials Letters, 59, 245 – 249

[6] Lo, S., Yang, C. (1997), "The Sintering Characteristics of Bi_20_3 Added MgO-CaO-Al_20_3-SiO_2 Glass Powder", Ceramics International, 24, 139-144

[7] Gil, V., Tartaj, J., Moure, C., Durán, P. (2005), "Sintering, microstructural development, and electrical properties of gadolinia-doped ceria electrolyte with bismuth oxide as a sintering aid", Journal of the European Ceramic Society, 26, 3161–3171

[8] Pooladvand, H., Baghshahi, S., Mirhadi, B., Souri, A.R., Arabi, H. (2011), "Effect of MgO and CaO on Transformation of Andalusite to Mullite", ASM International, 21:1637–1644

[9] Nour, W.M.N., Awad, H.M. (2008), "Effect of MgO on Phase Formation and Mullite Morphology of Different Egyptian Clays", Journal of the Australian Ceramic Society, 44[2], 27-37

[10] Rendtorff, N.M., Garrido, L.B., Aglietti, E.F. (2008), "Effect of the addition of mullite–zirconia to the thermal shock behavior of zircon materials", Materials Science and Engineering, 498, 208–215

[11] Bhagat, V., (2010), "Effect of TiO_2 as an additive on the phase formation and densification of mullite-zirconia composites", National Institute of Technology, Rourkela, Odisha, India

[12] Zhang, G., Fu, Z., Wang, Y., Wang, H., Wang, W., Zhang, J., Lee, S.W., Niihara, K. (2010), "Boron-doped mullite derived from single-phase gels", Journal of the European Ceramic Society, 30, 2435–2441

[13] Tripathi, H.S., Banerjee, G. (1998), "Synthesis and Mechanical Properties of Mullite from Beach Sand Sillimanite: Effect of TiO_2", Central Glass and Ceramic Research Institute

[14] Bisoyi, K. (2012), "Study of Zirconia-Mullite system: Effect of SrO addition with alumina content variation", National Institute of Technology, Rourkela, Odisha, India

[15] Viswabaskaran, V., Gnanam, F.D., Balasubramanian, M. (2003), "Effect of MgO, Y_2O_3 and boehmite additives on the sintering behaviour of mullite formed from kaolinite-reactive alümina", Journal of Materials Processing Technology, 142, 275–281

[16] Ouali, A., Heraiz, M., Sahnoune, F.,Belhouchet, H., Fatmi, M., Saheb, N. (2013), "Effect of MgO addition on the mechanical and thermal properties of mullite synthesised through reaction sintering of Al_2O_3 and Algerian kaolin", American Journal of Modern Physics, 2(5): 270-275

[17] Souto, P.M., Menezes, R.R., Kiminami, R.H.G.A. (2008), "Sintering of commercial mulite powder: Effect of MgO dopant", Journal of Materials Processing Technology, 209 (2009) 548–553, 209, 548–553

[18] Montanaro, L., Perrot, C., Esnouf, C., Thollet, G., Fantozzi, G., Negro A. (2000), "Sintering of Industrial Mullites in the Presence of Magnesia as a Sintering Aid", Journal of the American Ceramic Society, 83 [1] 189–96

CURRICULUM VITAE

Adı Soyadı : Sevnur ÖZDEMİR

Doğum Yeri ve Tarihi : Bulgaristan / 06.04.1984

Yabancı Dili : İngilizce, Almanca

E-Posta : sewnur@yahoo.com

Öğrenim Durumu

Derece	Bölüm/Program	Üniversite/Lise	Mezuniyet Yılı
Lise	Fen - Matematik	Gebze Anibal Anadolu Lisesi	2002
Üniversite	Metalurji Malz. Müh.	Marmara Üniversitesi	2008

İş Deneyimi

Yıl	Firma/Kurum	Görevi
2009-	Cam Elyaf San. A.Ş.	Laboratuvar Mühendisi